25th ABCM International Congress of Mechanical Engineering
October 20-25, 2019, Uberlândia, MG, Brazil

COB- 2019-0369

A NUMERICAL ANALYSIS OF THE MECHANICAL BEHAVIOR OF BONDED AND HYBRID JOINTS

Joseph Richard Pinheiro de Carvalho
Ricardo Alexandre Amar de Aguiar
Hector Reynaldo Meneses Costa
Pedro Manuel Calas Lopes Pacheco
CEFET/RJ, Av. Maracanã, 229 - Maracanã - RJ - CEP: 20271-110 - Brazil.
joseph.carvalho@aluno.cefet-rj.br
ricardo.aguiar@cefet-rj.br
hector.costa@cefet-rj.br
pedro.pacheco@cefet-rj.br

Juliana Primo Basílio de Souza
UFMG, Av. Antônio Carlos, 6627 - Pampulha, Belo Horizonte - MG - CEP: 31270-901 - Brazil.
juliana_basilio@demec.ufmg.br

Abstract. *The increasing demand for new technologies to improve products and reduce costs expand the usage of hybrid techniques to join materials in industry. This technique adds the benefits of two or more joining techniques to the material joint. The automotive and aerospace industry is using and developing the method for joining metallic thin sheets through hybrid welds, resulting from the combination of electrical resistance spot welding and bonding with structural adhesives. The present study has the objective of evaluating the mechanical behavior of single-lap joints manufactured by adhesive bonding, spot welding and a hybrid of both techniques using a numerical model based on the finite element method, simulating the shear test. The interstitial free steel (IF steel) was the material used as the adherent and Syntho-SubseaTM LV Epoxy was the material used as the adhesive. The simulations of adhesive and hybrid joints have considered the model of cohesive zone material (CZM), which allows simulating the behavior of adhesive´s rupture, using strength criteria and fracture mechanics concepts. It was possible to discuss the simulated results compared the previous experimental tests, and to examine the contribution of each type joint method in the hybrid joint strength. The results showed that the simulations were able to capture the main characteristics and effects of the experimental tests.*

Keywords: *CZM, Hybrid joint, Adhesive, Resistance Spot Welding, Single-Lap*

1. INTRODUCTION

The automotive industries are studying and applying hybrid welding to join two or plus metallic sheets. These methods have the purpose of reduce the fabrication cost of automobiles. The most used processes for the union those sheets in automotive industries are the resistance spot welding (RSW) and the use of adhesives. The RSW has been used in many industries, especially in the automotive and aerospace, due to its low cost, operation speed, localized heating and easiness of automation. Merging both processes, the generate joints take advantage of adhesive ductility and mechanical strength of the spot welding. It is possible to increase the mechanical resistance, fatigue resistance, corrosion resistance and improve mechanical energy absorption. The hybrid welding reduces the amount of welding points needed to maintain two metal sheets united. (Marques et al., 2016)

It is very difficult to predict with accuracy the reason of an adhesive joint failure. There are three types of failures: adhesion, cohesion and both. The adhesion failure occurs when the cohesive forces are greater than the interface forces. The cohesion failure occurs when the intermolecular forces are smaller than the bonding forces at the interface. The cohesion and adhesion failures occur together when the intermolecular forces and the interface forces are equivalent (Petrie, 2000, Da Silva et al., 2007).

A review of the numerical models using finite element analysis (FEA) for adhesive and hybrid joints made by He (2011), shows some methods to evaluate the different types and designs of joints. In addition, it presents the fracture failure modes evaluated by FEA. Recently, Budhea et al. (2017) did an excellent review of adhesively bonded joints, showing the mains numerical method and techniques to evaluate the behavior of different types of joints.

The objective of this work is to evaluate the mechanical behavior of three types of joints: adhesive, resistance spot welding and hybrid joints. Three numerical models will be formulated in ANSYS software, by finite element method

(FEM) and cohesive zone material (CZM) model, to represent the shear test of these joints. The shear tests analyzed and diagnosed which geometry parameters or material properties presented most influence in the mechanical behavior of the joints.

2. METHOD AND MATERIALS

The present study, has considered three models to evaluate three types of union process applied to joint of two Interstitial Free Steel (IF Steel) sheets. For this purpose, it was created a 3D model on ANSYS ® to represent the adhesive, spot welding and hybrid joints. These three models use FEM to calculate the mechanical resistance of the joints. However, in the adhesive and hybrid models, besides FEM, it was used the cohesive zone material (CZM) model.

The CZM is based on the fracture mechanics concepts including the start of failure by fracture resistance criteria. The fracture mechanics, considers three types of loads that generate the crack propagation: normal loads and shear forces in both axis.

CZM model can be used to characterize the constitutive behavior of the interface between two pieces. It is capable of representing the fracture mechanics or the delamination along the interface. This technique adopts softening relationships between traction loads and displacements that causes interface separations between two pieces. Through these traction and separation, it is possible to identify which critical fracture energy is necessary to separate two surfaces. The definitions of these loads depend on the element type and the material model.

ANSYS ® have two types of elements: interface and contact. In addition, three material models: exponential behavior, bilinear behavior and viscous regularization. The ANSYS (2015) have more details of how this elements types and materials models.

For this work, CZM was used based on mixed-mode (normal and tangential loads), contact element and bilinear behavior to represent the adhesive. According to ANSYS ® (2015), for mixed-mode debonding, both normal and tangential contact stresses contribute to the total fracture energy and debonding is completed before the critical fracture energy values are reached for the components. The curve and the equations of bilinear cohesive zone material behavior are shown in Fig.1.

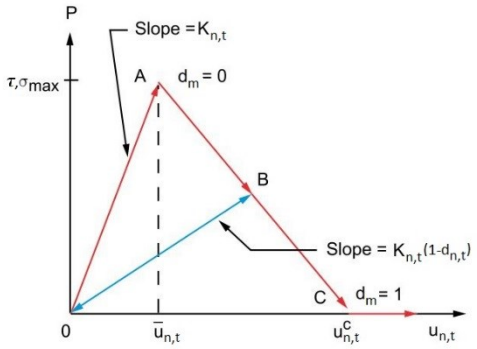

Figure 1. Contact stress and contact gap curve for bilinear cohesive zone material. (Ansys, 2015 - adapted)

The mixed mode debonding depends on both normal and tangential components. The normal contact stress (P), it is expressed by Eq. (1), and the tangential contact stress (τ_t) are governed by Eq. (2).

$$P = K_n u_n (1 - d_m) \tag{1}$$

Where:
K_n is the normal contact stiffness;
u_n is the contact gap;
d_m is the mixed debonding parameter.

$$\tau_t = K_t u_t (1 - d_m) \tag{2}$$

Where:
K_t is the tangential contact stiffness;
u_t is the tangential slip distance.

The debonding parameter in Mixed-Mode has a strong influence by the both components, normal and tangential contact stress. This parameter is defined as Eq. (3) and Eq. (4):

$$d_m = \left(\frac{\Delta_m - 1}{\Delta_m}\right)\chi, \text{ if } \Delta_m \leq 1 \rightarrow d_m = 0 \text{ and if } \Delta_m > 1 \rightarrow 0 < d \leq 1 \quad (3)$$

With $\Delta_m = \sqrt{\Delta_n^2 + \Delta_t^2}$; $\Delta_n = \frac{u_n}{\bar{u}_n}$ and $\Delta_t = \frac{u_t}{\bar{u}_t}$.

$$\chi = \left(\frac{u_n^c}{u_n^c - \bar{u}_n}\right) = \left(\frac{u_t^c}{u_t^c - \bar{u}_t}\right) \quad (4)$$

Where:

χ is a constraint based on the ratio of the contact gap distance, and it is the same as ratio of tangential slip distance. That consideration is applied scaling the contact stiffness value (K_t) as shown Eq. (5):

$$K_t = \left(\frac{\tau_{max} u_n^c}{\sigma_{max} u_t^c}\right) K_n \quad (5)$$

u_n^c is the critical normal contact gap, on this value occurs the completion of debonding;
$\bar{u}_n$ is the contact gap at the maximum normal contact stress;
u_t^c is the critical tangential slip distance, on this value occurs the completion of debonding;
$\bar{u}_t$ is the tangential slip distance at the maximum normal contact stress;

The normal critical fracture energy is the area value under the curve of Fig. 1 and it is calculated based the relationship of the maximum normal contact stress (σ_{max}) and the critical normal contact gap, as shown Eq. (6).

$$G_{cn} = \frac{1}{2}\sigma_{max} u_n^c \quad (6)$$

The tangential critical fracture energy is the area value under the curve of Fig. 1 and it is calculated based the relationship of the maximum tangential contact stress (τ_{max}) and the critical tangential slip distance, as shown Eq. (7).

$$G_{ct} = \frac{1}{2}\tau_{max} u_t^c \quad (7)$$

Therefore, a power law based energy criteria is used to define the completion of debonding, as shown in Eq. (8). With G_n and G_t being, as shown Eq. (9) respectively, the normal and tangential fracture energies at a specific point.

$$\left(\frac{G_n}{G_{cn}}\right)^2 + \left(\frac{G_t}{G_{ct}}\right)^2 = 1 \quad (8)$$

Where:

$$G_n = \int P du_n \text{ and } G_t = \int \tau_t du_t \quad (9)$$

According Costa et al. (2015), the shear tests were prepared in agreement to standard ASTM D 1002 and conducted with objective of determining the shear and direct tension strengths of the tested joints. The sheets, with dimensions of 25 x 135 x 0.75 mm, are composed IF Steel titanium-stabilized used in the experimental trials of Costa et al. (2015), they are coated by the hot immersion process with zinc at 60 [g/m²], 0.75 [mm] of thickness and density of 7860 [kg/m³], manufactured by CSN GALVASUD S/A. The mechanical properties of the IF Steel used in the experiments of Costa et al. (2015) are shown on Tab. 1. Costa et al. (2015) used the adhesive Syntho-Subsea ™LV Epoxy, provided by Neptune Research Inc., to produce the adhesive joint and hybrid joint with thickness 0.85 mm. The Table 2 shows the adhesive properties.

Table 1. Mechanical properties of IF steel (Costa et al., 2015).

Yield strength	Ultimate tensile stress	Elongation	Hardness	Roughness
182 MPa	296 MPa	43(%)	37 (HRB)	0.8-0.7 (μm)

Table 2. Adhesive properties (Costa et al., 2015)

Properties	Syntho-Subsea™ LV Epoxy
Flexural strength	31.4 MPa
Tensile strength	41.0 MPa
Compressive strength	50.9 MPa
Flexural modulus	980.0 MPa
Shear strength	12.3 MPa
Abrasion resistance	34mg/1000cy

3. FEM Models

Three numerical models are proposed in this study to represent three types of joints and analyses the behavior of the spot welding, adhesive and hybrid joints during shear test. The numerical simulations were performed by commercial code ANSYS (2015), which is based on finite elements method and allows configure the CZM technique.

For the adhesive and hybrid joints models, it was considered a bilinear material behavior with tractions and separation distances to set the adhesive parameters of the CZM in ANSYS®. The parameters are shown on Tab.3. The FEM models considered non-linear conditions: large displacements, material properties and contact elements.

Table 3. Principals' parameters of the simulations.

IF Steel	Adhesive
Material: Elastoplastic Bilinear Kinematic	Material: Bilinear Behavior
Element type: SOLID 186	Element type: TARGET 170 and CONTACT 174
-	Contact Models: CZM - contact element
Elastic modulus: 210 GPa	Maximum normal contact stress: 31 MPa
Poisson ratio: 0.29	Contact gap at the completion of debonding $4.2x10^{-3}$ mm
Yield stress: 190 MPa	Maximum equivalent tangential contact stress 12.3 MPa
Hardening parameter: 0.75 GPa	Tangential slip at the completion of debonding 1.5 mm

The dimension of the sheets and the overlap area were following according ASTM D 1002, where: L_o = 25mm, L_y=12.5 mm (considering symmetry), L_T = 245 mm and t_s = 0.75 mm (Fig. 2). Five meshes were generated with different sizes elements for each model. For the convergence analyses, two evaluations were made. The first evaluation was about the average size of the mesh element and the second one was about the time step.

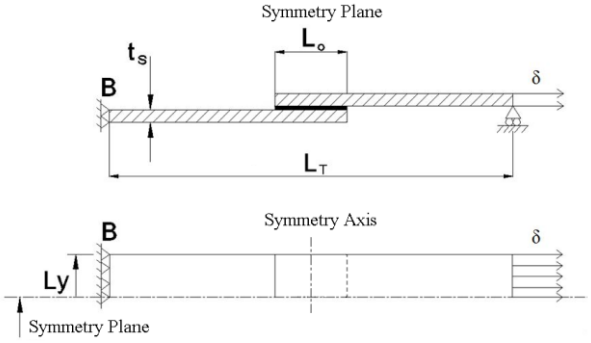

Figure 2. Boundary conditions scheme for Adhesive joint.

The Figure 2 shows the boundary conditions applied and dimensions for the adhesive joints. It was considering longitudinal symmetry; "B" is zero translation and rotation on three directions; δ is the prescript displacement. For the adhesive δ=1.6 mm, that value is an output data of the experimental shear test. The overlap area that represents the union between the sheets with adhesive is represented in the model by the contact element using the CZM technique.

The Figure 3 shows examples of the 3D FEM models used to do the mesh convergence analyses. For adhesive joint, it was considered contact elements on the overlap area of the sheets. For the resistance spot welding joints, it was considered a circular region to represent the nugget and make the union between the sheets, with all the nodes of both regions connected. And it was assumed that the nugget does not have any voids or failure, resulting by the welding process. For hybrid welding, the nugget it was represent as previously explained and for the rest of the overlapping area it was applied the contact elements to compose the bond area between the sheets.

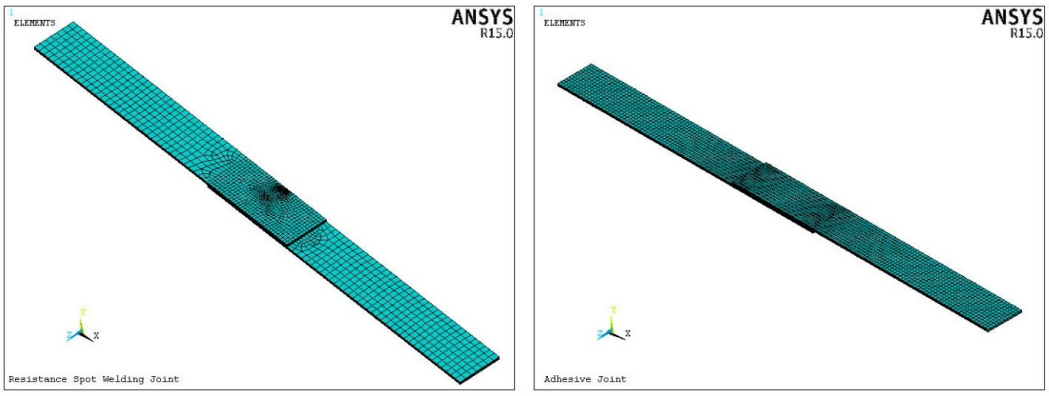

Figure 3. FEM models: RSW and Hybrid joints (left) and Adhesive joint (right).

The Figure 4 shows the boundary conditions applied for the both resistance spot welding and hybrid joints. It was considering longitudinal symmetry on S-S; "B" is zero translation and rotation on three directions; δ is the prescript displacement. For RSW models δ=8 mm for 4.0 mm of nugget diameter and δ=10 mm for 5.0 mm of nugget diameter. For Hybrid joint, were used the same condition of symmetry and constraints as used to others models. It was considerate the nugget diameter with 4.0 mm and δ=3.0 mm to identify the rupture effect on adhesive.

The Figure 5 shows the representative boundary conditions applied on the three FEM models. Where "U" represents the constraint of the displacement applied, "ROT" represents the rotation restriction applied and "CP" represents the nodes on which the prescribed displacement is applied.

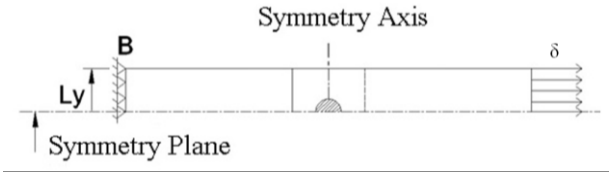

Figure 4. Boundary conditions scheme for Spot Welding and Hybrid joints.

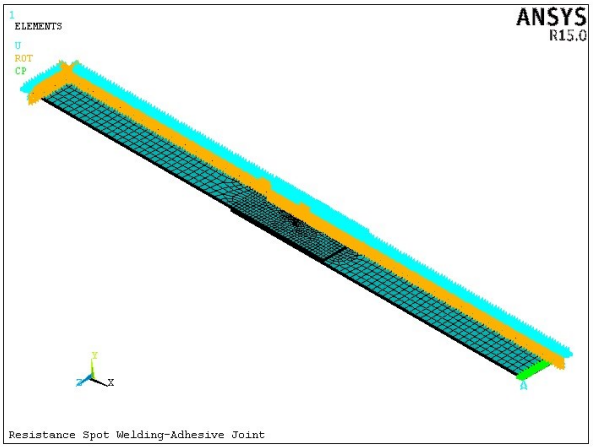

Figure 5. Boundary conditions applied on the three models.

After the mesh convergence analysis it was defined the three meshes of FEM models to make the simulations. A mesh with 14,669 elements and 62,232 nodes was used for the adhesive joints model. The mesh of the resistance spot welding model with 4 mm of nugget diameter has 13,593 elements and 57,406 nodes and for 5 mm of nugget diameter has 13,849 elements and 57,986 nodes. And for the Hybrid model it was used a 13,490 elements and 52,438 nodes mesh. Table 3 shows the element types and the parameters of the simulations. After a convergence analysis, the prescribed displacement was applied in X direction, considering equally spaced time subdivisions for each models. For adhesive joint, it was applied 40 time subdivisions, for resistance spot weld it was used 35 time subdivisions for both nugget diameters and for hybrid joint 40 time subdivisions.

4. RESULTS

The results of shear test simulation were compared with experimental results of Costa et al. (2015). It was noted that the results shows that the FEM model has a great potential to represent the three proposed models, even though there is a great difficulty in calibrating the adhesive models. The Figure 6 shows the comparison between the experimental and the best simulated results for the three models.

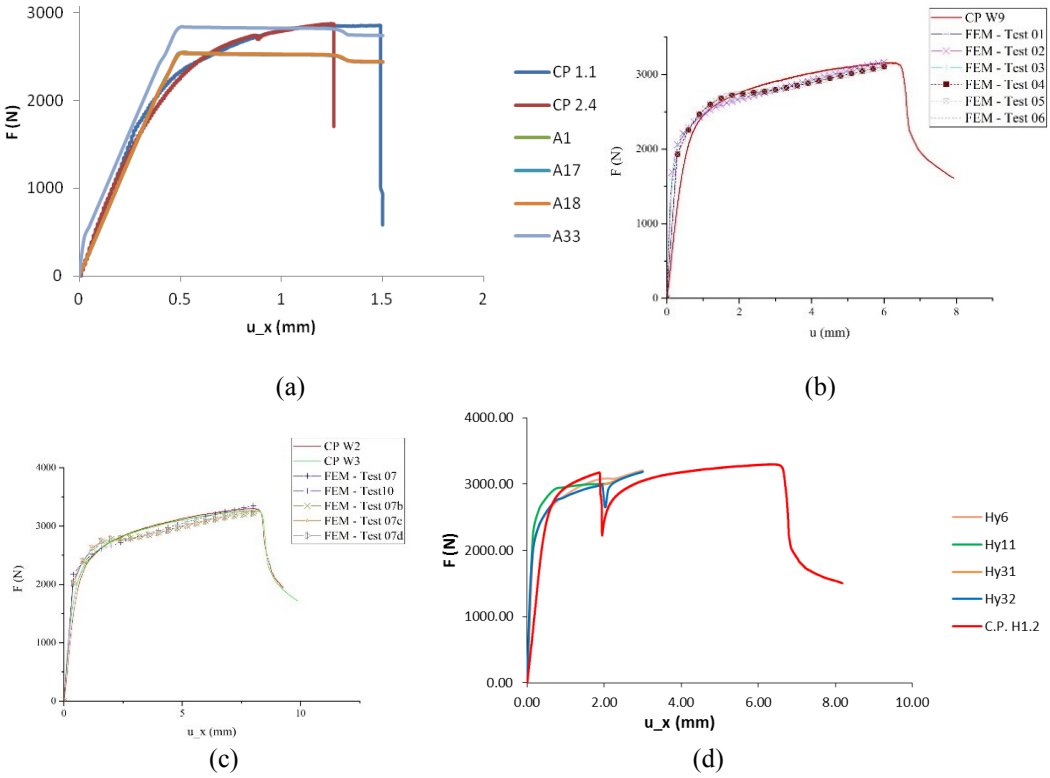

Figure 6. Comparison between experimental and simulated shear tests. (a) Adhesive joints; (b) and (c) RSW joints; (d) hybrid joints.

The simulation cases made for adhesive joints; those cases have a prescript displacement of 1.5 mm. It is possible to verify, at Fig. 6-a, that the cases A1, A17 and A18 have reasonable approximations of the stiffness that the test subjects presented in the experiment (CP 1.1 and CP 2.4) of Costa et al. (2015). The maximum load achieved by the experiment was 2860 N. The case A33 was close to the force level of 2835.65 N. However, at the beginning of the crack propagation and the debonding, the achieved force was kept stable up to the beginning of the force reduction, suggesting a new rupture in the interface. To capture the adhesive rupture, the model requires more experimental data for calibration.

The simulation cases generated for RSW joints, considering 4.0 mm of the nugget diameter and an average maximum load result of 3160 N (CP W9) and 5.0 mm of the nugget diameter with an average maximum load of 3287 N (CP W2 and CP W3). It is possible to verify that in the cases FEM – test 01(Fig. 6-b) and FEM – test 07 (Fig. 6-c) the maximum force level gets close of the experimental test, as an indication of a good accuracy of the numeric model. The maximum load of FEM01 case is 3162.92 N and for the FEM07 case, it is 3349.57 N.

The Figure 7 shows the von Mises equivalent stress distribution for a representative example of cases simulated for a RSW with 4mm diameters, where is presented a real scale for the displacement. The region near the nugget shows, in red, a stress concentration. It is possible to identify larges values of displacement, stress and plastic strain.

The Figure 8 shows a comparison between FEM model proposed and experimental work of the Costa et al. (2015) for the RSW joint. The FEM models of resistance spot welding joints were capable of capturing the main effects of the shear test.

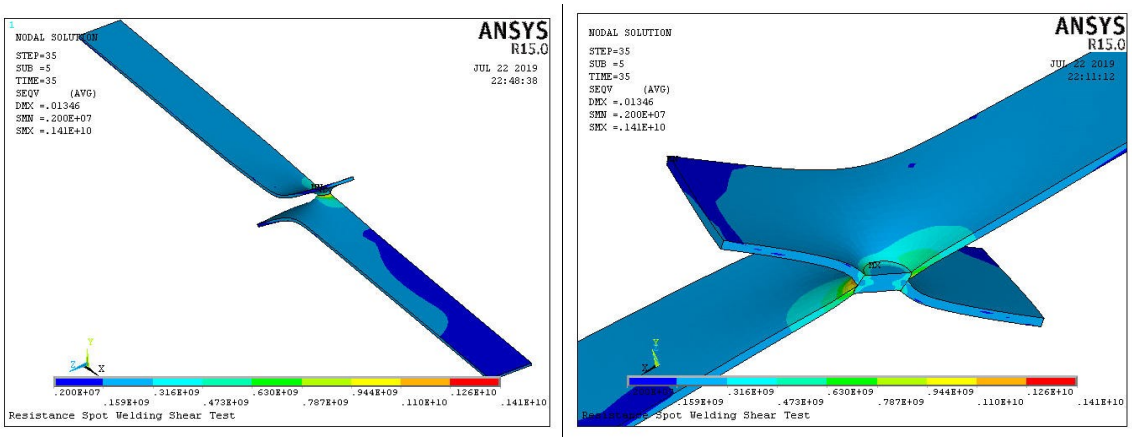

(a) (b)

Figure 7. Resistance Spot Welding Joint: (a) von Mises equivalent stress distribution, (b) detail of the nugget welding.

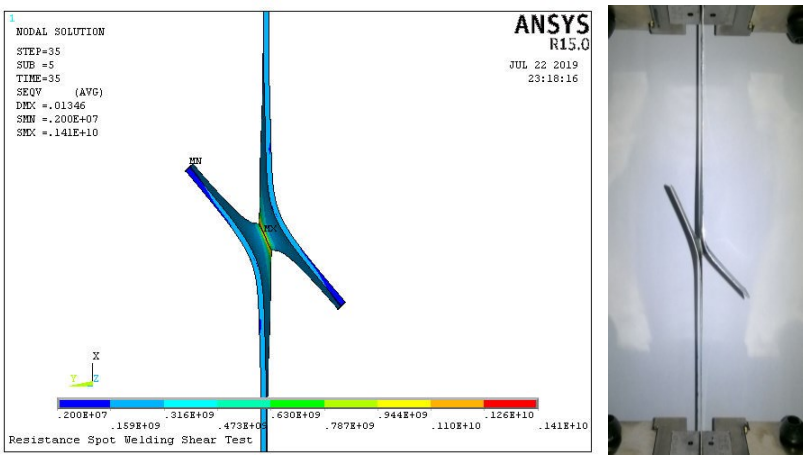

Figure 8. Resistance Spot Welding Joint: (left) FEM Model and (right) Experimental of Costa et al. (2015) results.

The simulation cases generated for Hybrid joints with prescript displacement of 3 mm. The case Hy32 (Fig. 6-d) achieved the closest comportment from the experimental test. The main difficulty of this kind of analysis is being able to capture the rupture of the adhesive with an abrupt reduction of force and the return of increase loading through the resistance that the spot welding provides. The average maximum load upholds by the hybrid joint before the adhesive rupture on the experiment was of 3175 N. At the numerical model, for the same region, this value was of 2989.02 N.

The Figure 9 (a), (b) and (c) shows the debonding parameters for the hybrid model. Fig. 9 (d) shows the von Mises equivalent stress distribution. It indicates that the start of the debonding occurs near the nugget because of a stress concentration in this region.

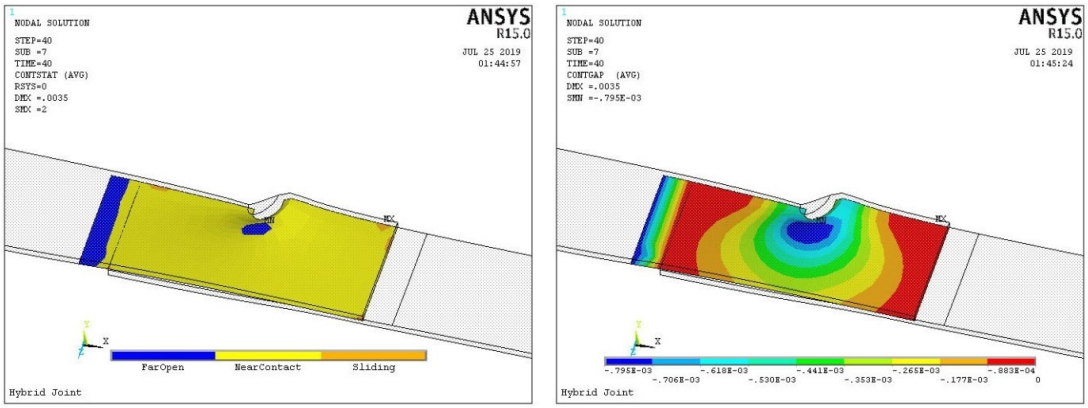

(a) (b)

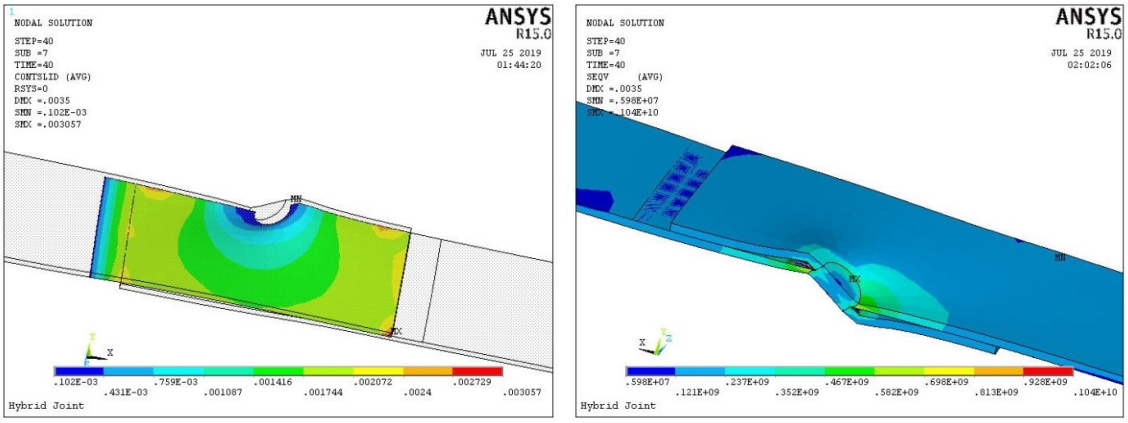

(c) (d)

Figure 9. Debonding Parameters of the Hybrid Joint: (a) Status, (b) Contact Gap, (c) Sliding distances and (d) von Mises equivalent stress distribution.

Souza et al. (2018) used Costa et al. (2015) experiments to validate a numerical by prescribed displacement model for RSW and hybrid joints. When comparing the numerical results of the model of Souza et al. (2018) with the model realized in the present work, it is possible to note that the results show consistency. Therefore, the results showed that the models were able to capture the main characteristics and effects of the experimental tests.

5. CONCLUSIONS

The results of adhesive model show that the model of this simulation requires more experimental data to calibrate the model. The proposed models for resistance spot welding and hybrid joints had a good accuracy of the numeric model. Even thought the limitations of the models, they were able to indicate the main characteristics of the joints when submitted to the shear test. Therefore, the studies showed that this methodology is indicated to evaluate joints of resistance spot welding and hybrid welding. For future work, it will propose the use of different kinds of adhesive to do experimental shear tests and calibrate those models.

6. ACKNOWLEDGEMENTS

The authors acknowledge the support of the Brazilian Research Agencies Conselho Nacional de Desenvolvimento Científico e Tecnológico (CNPq) and Coordenação de Aperfeiçoamento de Pessoal de Nível Superior (CAPES).

7. REFERENCES

ANSYS ®, 2013. "User Manual, Release - 15.0 - Help System", ANSYS, Inc.

ASTM D1002–10 Standard Test Method for Apparent Shear Strength of Single-Lap-Joint Adhesively Bonded Metal Specimens by Tension Loading (Metal-to-Metal).

Budhea, S., Baneaa, M. D., de Barrosa, S. and da Silva L.F.M., 2017, "An updated reviwe of adhesively bonded joints in composite materials", *International Journal Adhesion and Adhesive,* Vol.72, pp.30-42.

Costa, H. R. M., Reis, J. M. L., Souza, J. P. B., Pacheco, P . M. C. L., Aguiar, R. A. A. and De Barros, S., 2015. "Experimental investigation of the mechanical behaviour of spot welding–adhesives joints", *Composite Structures*, Elsevier, Vol. 133, pp. 847-852.

Da Silva, L.F.M., De Magalhães, A.G. and De Moura, M.F.S.F., 2007, Juntas Adesivas Estruturais, *Publindústria*, Porto.

He, X., 2011. "A review of finite element analysis of adhesively bond joints", *International Journal of Adhesion & Adhesives, Elsevier*, Vol. 31, pp.248-264.

Marques, G.P., Campilho, R.D.S.G., Da Silva, F.J.G. and Moreira, R.D.F., 2016. "Adhesive selection for hybrid spot-welded/bonded single-lap joints: Experimentation and numerical analysis", C*omposites Part B: Engineering, Elsevier*, Vol. 84, pp. 248-257.

Petrie, E.M., 2000. Handbook of Adhesives and Sealants, McGraw-Hill, New York.1st edition.

Souza, J.P.B., Aguiar, R.A.A., Costa, H.R.M., Reis, J.M.L. and Pacheco, P.M.C.L., 2018. "Numerical modelling of the mechanical behavior of hybrid joint obtained byspot welding and bonding", *Composites Structure*s, Vol. 202, pp. 216-221.

8. RESPONSIBILITY NOTICE

The author(s) is (are) the only responsible for the printed material included in this paper.